February 19, 2015 - Version: after Collaboration

An improved limit to the diffuse flux of ultra-high energy neutrinos from the Pierre Auger Observatory

The Pierre Auger Collaboration
Observatorio Pierre Auger, Av. San Martín Norte 304, 5613 Malargüe, Argentina *

Neutrinos in the energy range around 1 EeV and above can be detected with the Surface Detector array (SD) of the Pierre Auger Observatory. They can be identified through the broad time-structure of the signals expected to be induced in the SD stations. The identification can be efficiently done for neutrinos of all flavours interacting in the atmosphere at large zenith angles, typically above 60° (downward-going), as well as for "Earth-skimming" neutrino interactions in the case of tau neutrinos (upward-going). The wide angular range calls naturally for three sets of identification criteria designed to search for downward-going neutrinos in the zenith angle bins $60^\circ - 75^\circ$ and $75^\circ - 90^\circ$ as well as for upward-going neutrinos. In this paper the three searches are combined to give a single limit, providing, in the absence of candidates in data from 1 January 2004 until 20 June 2013, an updated and stringent limit to the diffuse flux of ultra-high energy neutrinos. The sensitivity has improved with respect to the latest published results due to the additional data, the combination of the Earth-Skimming and downward-going searches, and the improved calculation of the exposure to UHE neutrinos.

PACS numbers: 95.55.Vj, 95.85.Ry, 98.70.Sa
Keywords: Ultra-high-energy cosmic rays and neutrinos, high-energy showers, ground detector arrays, Pierre Auger Observatory

I. INTRODUCTION

The flux of ultra-high energy cosmic rays (UHECRs) above $\sim 5 \times 10^{19}$ eV is known to be suppressed with respect to that extrapolated from lower energies. This feature has been seen in the UHECR spectrum [1, 2], with the position of the break being compatible with the Greisen-Zatsepin-Kuzmin (GZK) effect [3], i.e. the interaction of UHECRs with the cosmic microwave background (CMB) radiation. However, other explanations are possible, most prominently a scenario where the limiting energy of the UHECR sources is being observed [4]. Key to distinguishing between these two scenarios is the determination of the composition of the UHECRs [5, 6], with the second scenario predicting increasing fractions of primaries heavier than protons as energy increases [4].

Above $\sim 5 \times 10^{19}$ eV cosmic-ray protons interact with CMB photons and produce ultra-high energy *cosmogenic* neutrinos of energies typically 1/20 of the proton energy [7]. Their fluxes are however uncertain and at EeV energies they depend mostly on the evolution with redshift z of the unknown sources of UHECRs, on the spectral features at injection, and most importantly on the nature of the primaries, with protons typically producing larger fluxes than heavier nuclei [8, 9]. In this respect the observation of UHE neutrinos can provide further hints on the dominant scenario of UHECR production [9], as well as on the evolution with z of their sources which can help in their identification [9, 10].

UHE neutrinos are also expected to be produced in the decay of charged pions created in the interactions of cosmic rays with matter and/or radiation at their potential sources, such as Gamma-Ray Bursts or Active Galactic Nuclei among others [11]. In fact, at tens of EeV, neutrinos may be the only direct probe of the sources of UHECRs at distances farther than ~ 100 Mpc.

A breakthrough in the field was the recent detection with the IceCube experiment of three neutrinos of energies just above 1 PeV, including a 2 PeV event which is the highest-energy neutrino interaction ever observed, followed by tens of others above ~ 30 TeV representing a $\sim 5.7\,\sigma$ excess above atmospheric neutrino background [12]. The measured flux is close to the Waxman-Bahcall benchmark flux [13], although with a steeper spectrum [36].

In the EeV energy range, i.e. about three orders of magnitude above the most energetic neutrinos detected in IceCube, neutrinos have so far escaped the scrutinity of existing experiments. These can be detected with a variety of techniques [14], among them with arrays of particle detectors at ground.

In this work we report on the search for EeV neutrinos in data taken with the Surface Detector array (SD) of the Pierre Auger Observatory [15]. A blind scan of data from 1 January 2004 up to 20 June 2013 has yielded no neutrino candidates and an updated and stringent limit to the diffuse flux of UHE neutrino flux has been obtained.

* auger_spokespersons@fnal.gov

II. SEARCHING FOR UHE NEUTRINOS IN AUGER

The concept for identification of neutrinos is rather simple. While protons, heavier nuclei, and even photons interact shortly after entering the atmosphere, neutrinos can initiate showers close to the ground level. At large zenith angles the atmosphere is thick enough so that the electromagnetic component of nucleonic cosmic rays gets absorbed and the shower front at ground level is dominated by muons ("old" shower front). On the other hand, showers induced by neutrinos deep in the atmosphere have a considerable amount of electromagnetic component at the ground ("young" shower front). The Surface Detector array (SD) of the Pierre Auger Observatory is not directly sensitive to the muonic and electromagnetic components of the shower separately, nor to the depth at which the shower is initiated. In the $\sim$1600 water-Cherenkov stations of the SD of the Pierre Auger Observatory, spread over an area of $\sim$3000 km^2, separated by 1.5 km and arranged in a triangular grid, the signals produced by the passage of shower particles are digitised with a FADC with 25 ns resolution. This allows us to distinguish narrow signals in time induced by inclined showers initiated high in the atmosphere, from the broad signals expected in inclined showers initiated close to the ground.

Applying this simple idea, with the SD of the Pierre Auger Observatory [15] we can efficiently detect inclined showers and search for two types of neutrino-induced showers at energies around EeV and above:

1. Earth-skimming (ES) showers induced by tau neutrinos (ν_τ) that travel in the upward direction with respect to the vertical to ground. ν_τ can skim the Earth's crust and interact relatively close to the surface inducing a tau lepton which escapes the Earth and decays in flight in the atmosphere, close to the SD.

   Typically, only Earth-skimming ν_τ -induced showers with zenith angles $90^\circ < \theta < 95^\circ$ may be identified.

2. Showers initiated by any neutrino flavour moving down at large angles with respect to the vertical at ground that interact in the atmosphere close to the surface detector array through charged-current (CC) or neutral-current (NC) interactions. We include here showers induced by ν_τ interacting in the mountains surrounding the Pierre Auger Observatory. Although this latter process is exactly equivalent to the "Earth-skimming" mechanism, it is included in this class because such showers are also going downwards. In the following we will refer to all these types of showers as "downward-going" (DG) ν-induced showers.

   With the aid of Monte Carlo simulations we have established that this search can be performed efficiently as long as it is restricted to showers with zenith angles $\theta > 60^\circ$. Due to the characteristics of these showers depending on the zenith angle, the search in this channel was performed in two angular subranges: (a) "low" zenith angle (DGL) corresponding to $60^\circ < \theta < 75^\circ$ and (b) "high" zenith angle (DGH) with $75^\circ < \theta < 90^\circ$.

A. General strategy

The identification of potential neutrino-induced showers is based on first selecting those events that arrive in inclined directions with respect to the vertical, and then selecting among them those with FADC traces that are spread in time, indicative of the early stage of development of the shower and a clear signature of a deeply interacting neutrino triggering the SD.

First of all, events occurring during periods of data acquisition instabilities [16] are excluded. For the remaining events the FADC traces of the triggered stations are first "cleaned" to remove accidental signals [17] induced (mainly) by atmospheric muons arriving closely before or after the shower front. These muons are typically produced in lower energy showers (below the energy threshold of the SD of the Auger Observatory) that arrive by chance in coincidence with the triggering shower. A procedure to select the stations participating in the event described in [17, 18] is then applied, with the event accepted if the number of accepted stations $N_{\rm st}$ is at least three (four) in the Earth-skimming (downward-going) selections.

From the pattern (footprint) of stations at ground a length L along the arrival direction of the event and a width W perpendicular to it characterizing the shape of the footprint can be extracted [17]. The ratio $L/W \sim 1$ in vertical events increasing gradually as the zenith angle increases. Very inclined events typically have elongated patterns on the ground along the direction of arrival and hence large values of L/W. A cut in L/W is therefore a good discriminator of inclined events. Another indication of inclined events is given by the apparent speed V of the trigger from a station i to a station j, averaged over all pairs (i, j) of stations in the event. This observable denoted as $\langle V\rangle$ is obtained from the distance between the stations after projection along L and from the difference in trigger times of the stations. In vertical showers $\langle V\rangle$ exceeds the speed of light since all triggers occur at roughly the same time, while in very inclined events $\langle V\rangle$ is concentrated around the speed of light. Moreover its Root-Mean-Square (RMS(V)) is small. For downward-going events only, a cut on the reconstructed zenith angle $\theta_{\rm rec}$ is applied [18].

Once inclined showers are selected the next step is to identify young showers. From the observational point of view, a Time-over-Threshold (ToT) trigger[1] is usually present in SD stations with signals extended in time, while narrow signals induce other local triggers. Also the Area-over-Peak ratio (AoP), defined as the ratio of the integral of the FADC trace to its peak value, normalized to 1 for the average signal produced by a single muon, provides an estimate of the spread-in-time of the traces, and serves as an observable to discriminate broad from narrow shower fronts. In particular, a cut on AoP allows the rejection of background signals induced by inclined hadronic showers, in which the muons and their electromagnetic products are concentrated within a short time interval, exhibiting AoP values close to the one measured in signals induced by isolated muons. These observables are used by themselves in the search for ν candidates, or combined in a linear Fisher-discriminant polynomial depending on the selection as described later in this work.

As a general procedure and to optimize the numerical values of the cuts and tune the algorithms needed to separate neutrino-induced showers from the much larger background of hadronic showers, we divided the whole data sample (1 January 2004 - 20 June 2013) into two parts (excluding periods of array instability). A selection dependent fraction of the data (*training period*), along with Monte Carlo simulations of UHE neutrinos, is dedicated to define the selection algorithm, the most efficient observables and the value of the cuts on them. These data are assumed to be overwhelmingly constituted of background showers. The applied procedure is conservative because the presence of neutrinos in the training data would result in a more severe definition of the selection criteria. The remaining fraction of data is not used until the selection procedure is established, and then it is "unblinded" to search for neutrino candidates. We used real data to train the selections instead of Monte Carlo simulations of hadronic showers, the primary reason being that the detector simulation may not account for all possible detector defects and/or fluctuations that may induce events that constitute a background to UHE neutrinos, while they are contained in data. It is important to remark that this is the same selection procedure and training period as in previous publications [17, 18], which is applied in this work to a larger data set.

Regarding the Monte Carlo simulations, the phase space of the neutrino showers reduces to three variables: the neutrino energy E_ν, the incidence zenith angle θ and the interaction depth D in the atmosphere for downward-going neutrinos, or the altitude h_c of the τ decay above ground in the case of Earth-skimming neutrinos. Showers were simulated with energies from $\log(E_\tau/\mathrm{eV}) = 17$ to 20.5 in steps of 0.5, zenith angles from $90.1°$ to $95.9°$ in steps of 0.01 rad (ES) and from $60°$ to $90°$ in steps of 0.05 rad (DG). The values of h_c range from 0 to 2500 m (in steps of 100 m) whereas D is uniformly distributed along the shower axis in steps of 100 g cm^{-2}.

We have described the general strategy to search for Earth-skimming ν_τ and downward-going ν-induced showers. However the two searches (ES and DG) differ in several aspects that we describe in the following sections.

B. Earth-skimming neutrinos

With Monte Carlo simulations of UHE ν_τ propagating inside the Earth, we have established that τ leptons above the energy threshold of the SD are efficiently produced only at azimuth angles between $90°$ and $95°$. For this reason, in the Earth-skimming analysis we place very restrictive cuts on L/W, $\langle V\rangle$ and RMS(V), to select only quasi-horizontal showers with largely elongated footprints: $L/W > 5$ and $\langle V\rangle \in [0.29, 0.31]$ m ns^{-1} with RMS(V)< 0.08 m ns^{-1} (see Table I)[2].

In the ES selection, the neutrino identification variables include the fraction of stations with ToT trigger and having AoP> 1.4 for data prior to 31 May 2010 [17] being required to be above 60% of the triggered stations in the event. The final choice of the values of these cuts was made by requiring zero background events in the training data sample, corresponding to 1% of the events recorded up to that date. For data beyond 1 June 2010 a new methodology and a new set of efficient selection criteria was established based on an improved and enlarged library of ES simulated ν_τ events and on a larger period of training data. In particular, we used the average value of AoP ($\langle$AoP$\rangle$) over all the triggered stations in the event as the main observable to discriminate between hadronic showers and ES neutrinos. The new methodology allows us to place the value of the cut on $\langle$AoP$\rangle$ using the tail of its distribution as obtained in real data (which was seen to be consistent with an exponential shape as shown in Fig. 1). This tail was fitted and extrapolated to find the value of the cut corresponding to less than 1 expected event per 50 yr on the full SD array. As a result, an event is tagged as a neutrino candidate if $\langle$AoP$\rangle > 1.83$ (see Table I and Fig. 1). The new methodology is not applied to the data prior to 31 May 2010 since that data period was already unblinded to search for UHE neutrinos under the older cuts [17].

Roughly $\sim$ 95% of the simulated inclined ν_τ events producing τ leptons above the energy threshold of the SD

[1] This trigger is intended to select sequences of small signals in the FADC traces spread in time. It requires at least 13 bins in 120 FADC bins of a sliding window of 3 μs above a threshold of 0.2 I^{peak}_{VEM} (the peak value of the signal expected for a vertical muon crossing the station), in coincidence in 2 out of 3 PMTs [16].

[2] The axis of Earth-skimming showers travelling in the upward direction does not intersect the ground, contrary to the case for downward-going showers. For this reason, we exploit the properties of the footprint generated by the shower particles that deviate laterally from the shower axis and trigger the SD water-Cherenkov stations.

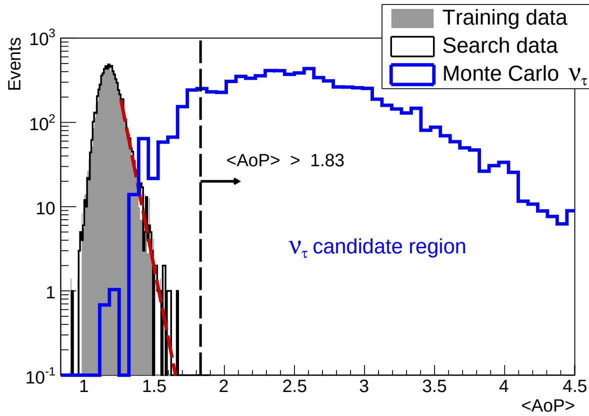

Figure 1. Distributions of $\langle\mathrm{AoP}\rangle$ (the variable used to identifiy neutrinos in the ES selection for data after 1 June 2010) after applying the inclined shower selection in Table I. Gray-filled histogram: the data in the training period. Black histogram: data in the search period. These two distributions are normalised to the same number of events for comparison purposes. Blue histogram: simulated ES ν_τ events. The dashed vertical line represents the cut on $\langle\mathrm{AoP}\rangle > 1.83$ above which a data event is regarded as a neutrino candidate. An exponential fit to the tail of the distribution of training data is also shown as a red dashed line (see text for explanation).

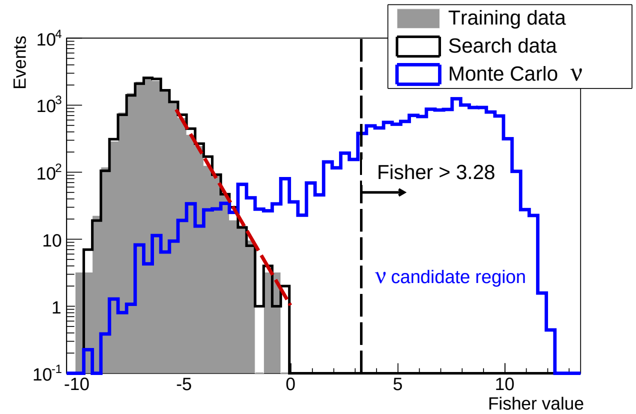

Figure 2. Distributions of the Fisher variable $\mathcal{F}$ in inclined events selected by the "Inclined Showers" DGH criteria in Table I, before applying the "Young Showers" cuts. In particular the distribution of events with number of triggered tanks $7 \leq\ N_{\rm st}\ \leq 11$ is shown. Gray-filled histogram: data in the training period corresponding to $\sim$ 23% of the whole data sample between 1 January 2004 and 20 June 2013. Black thin line: data in the search period. The distributions are normalised to the same number of events for comparison purposes. Blue line: simulated DGH ν events. The dashed vertical line represents the cut on $\mathcal{F} > 3.28$ above which a data event is regarded as a neutrino candidate. The red dashed line represents an exponential fit to the tail of the training distribution (see text for explanation).

are kept after the cut on $\langle\mathrm{AoP}\rangle$. The search for neutrinos is clearly not limited by background in this channel.

C. Downward-going neutrinos

In the high zenith angle range of the downward-going analysis (DGH) the values of the cuts to select inclined events are obtained in Monte Carlo simulations of events with $\theta > 75°$. Due to the larger angular range compared to Earth-skimming ν_τ, less stringent criteria are applied, namely $L/W > 3$, $\langle V\rangle < 0.313$ m ns^{-1}, RMS$(V)/\langle V\rangle <$ 0.08 plus a further requirement that the reconstructed zenith angle $\theta_{\rm rec} > 75°$ (see [18] and Table I for full details).

In the low zenith angle range corresponding to $60° < \theta < 75°$, L/W, $\langle V\rangle$ and RMS$(V)/\langle V\rangle$ are less efficient in selecting inclined events than the reconstructed zenith angle $\theta_{\rm rec}$, and for this reason only a cut on $\theta_{\rm rec}$ is applied, namely $58.5° < \theta_{\rm rec} < 76.5°$, which includes some allowance to account for the resolution in the angular reconstruction of the simulated neutrino events.

After the inclined shower selection is peformed, the discrimination power is optimized with the aid of the multivariate Fisher discriminant method [19]. A linear combination of observables is constructed which optimizes the separation between background hadronic inclined showers occuring during the downward-going training period, and Monte Carlo simulated ν-induced showers. The method requires as input a set of observables. For that purpose we use variables depending on the dimensionless Area-over-Peak (AoP) observable – as defined above – of the FADC traces.

In the DGH channel, due to the inclination of the shower the electromagnetic component is less attenuated at the locations of the stations that are first hit by a deep inclined shower (*early stations*) than in the stations that are hit last (*late stations*). From Monte Carlo simulations of $\nu-$induced showers with $\theta > 75°$ we have established that in the first few early stations the typical AoP values range between 3 and 5, while AoP tends to be closer to 1 in the late stations. Based on this simple observation and as already reported in [18], we have found a good discrimination when the following ten variables are used to construct the linear Fisher discriminant variable $\mathcal{F}$: the AoP and (AoP)^2 of the four stations that trigger first in each event, the product of the four AoPs, and a global parameter that measures the asymmetry between the average AoP of the early stations and those triggering last in the event (see [18] for further details and Table I).

The selection of neutrino candidates in the zenith angle range $60° < \theta < 75°$ (DGL) is more challenging since the electromagnetic component of background hadronic showers at ground increases as the zenith angle decreases because the shower crosses less atmosphere before reaching the detector level. Out of all triggered stations of an event in this angular range, the ones closest to the shower core exhibit the highest discrimination power in terms of AoP. In fact it has been observed in Monte Carlo simulations that the first triggered stations can still contain some electromagnetic component for background events and, for this reason, it is not desirable to use them for discrimination purposes. The last ones, even if they are triggered only by muons from a background hadronic shower, can exhibit large values of AoP because they are far from the core where muons are known to arrive with a larger spread in time. Based on the information from Monte Carlo simulations, the variables used in the Fisher discriminant analysis are the individual AoP of the four or five stations (depending on the zenith angle) closest to the core, and their product [20]. In the DGL analysis it is also required that at least 75% of the triggered stations closest to the core have a ToT local trigger [20].

Once the Fisher discriminant $\mathcal{F}$ is defined, the next step is to define a numerical value $\mathcal{F}_{\rm cut}$ that efficiently separates neutrino candidates from regular hadronic showers. As was done for the variable $\langle \mathrm{AoP} \rangle$ in the Earth-skimming analysis, $\mathcal{F}_{\rm cut}$ was fixed using the tail of the distribution of $\mathcal{F}$ in real data, which is consistent with an exponential shape in all cases. An example is shown in Fig. 2. The tail was fitted and extrapolated to find the value of $\mathcal{F}_{\rm cut}$ corresponding to less than 1 expected event per 50 yr on the full SD array [18, 20]. Roughly $\sim 85\%$ ($\sim 60\%$) of the simulated inclined ν events are kept after the cut on the Fisher variable in the DGH (DGL) selections. The smaller efficiencies for the identification of neutrinos in the DGL selection are due to the more stringent criteria in the angular bin $\theta \in (60^\circ, 75^\circ)$ needed to reject the larger contamination from cosmic-ray induced showers.

III. DATA UNBLINDING AND EXPOSURE CALCULATION

A. Data unblinding

No events survived when the Earth-skimming and downward-going selection criteria explained above and summarized in Table I are applied blindly to the data collected between 1 January 2004 and 20 June 2013. For each selection the corresponding training periods, are excluded from the search. After the unblinding we tested the compatibility of the distributions of discriminating observables in the search and training samples. Examples are shown in Fig. 1 for the $\langle \mathrm{AoP} \rangle$ variable in the Earth-skimming analysis, and in Fig. 2 for the Fisher variable in the DGH analysis. In particular fitting the tails of the corresponding distributions to an exponential, we obtained compatible parameters within 1 σ statistical uncertainties.

B. Exposure calculation

1. *Neutrino identification efficiencies*

The same set of criteria indicated in Table I, were also applied to neutrino-induced showers simulated with Monte Carlo, and the fraction of simulated events identified as neutrino candidates i.e. the identification efficiencies $\epsilon_{\rm ES}$, $\epsilon_{\rm DGH}$, $\epsilon_{\rm DGL}$ for each channel were obtained, necessary ingredients for the calculation of the exposure to UHE neutrinos.

A large set of Monte Carlo simulations of neutrino-induced showers was performed for this purpose, covering the whole parameter space where the efficiency is expected to be sizeable. In the case of Earth-skimming ν_τ induced showers, the efficiency depends on the energy of the emerging τ leptons E_τ, on the zenith angle θ and on the altitude of the decay point of the τ above ground X_d. These efficiencies are averaged over azimuthal angle and the τ decay channels. The maximum efficiency that can be reached is 82.6%, the 17.4% remaining corresponds to the channel in which the τ decays into a μ which is unlikely to produce a detectable shower close to ground. In the case of downward-going neutrinos the identification efficiency depends on neutrino flavour, type of interaction (CC or NC), neutrino energy E_ν, zenith angle θ, and distance D measured from ground along the shower axis at which the neutrino is forced to interact in the simulations.

The identification efficiencies depend also on time, through the changing configuration of the SD array that was growing steadily since 2004 up to 2008, and because the fraction of working stations - although typically above 95% - is changing continuously with time. Also the continuous monitoring of the array reveals a slight evolution with time of the optical properties of the water-Cherenkov stations (see below). Although the number of working stations and their status are monitored every second and as a consequence the SD configuration is known with very good accuracy at any instant of time, in practice, to avoid having to cope with an unaffordable number of configurations, different strategies were devised to calculate in an accurate and less time-consuming manner the actual identification efficiencies (as explained in [17, 18, 20]).

The evolution of the optical properties of the water-Cherenkov stations was taken into account in an effective way in the calculation of the exposure. The main effect of this evolution is a decrease with time of the decay time of the light as obtained from the monitoring data that revealed a continuous decrease of $\sim 10\%$ from 2004 until the end of the data period used in this work (20 June 2013). This induces a reduction of the AoP and, as a consequence, the trigger efficiency changes with time. These changes were accounted for in the calculation of the exposure by dividing the whole data set into three separate periods and assuming that in each of them the decay time of the light in the tank remained approximately constant as seen in data. A conservative approach was adopted by choosing constant values of the light decay time below the actual curve in the three periods.

Selection	Earth-skimming (ES)	Downward-going *high* angle (DGH)	Downward-going *low* angle (DGL)
Flavours & Interactions	ν_τ CC	$\nu_e,\ \nu_\mu\ ,\nu_\tau$ CC & NC	$\nu_e,\ \nu_\mu\ ,\nu_\tau$ CC & NC
Angular range	$\theta > 90°$	$\theta \in (75°, 90°)$	$\theta \in (60°, 75°)$
N° of Stations ($N_{\rm st}$)	$N_{\rm st} \geq 3$	$N_{\rm st} \geq 4$	$N_{\rm st} \geq 4$
	–	$\theta_{\rm rec} > 75°$	$\theta_{\rm rec} \in (58.5°,\ 76.5°)$
Inclined	$L/W > 5$	$L/W > 3$	–
Showers	$\langle V \rangle \in (0.29,\ 0.31)$ m ns^{-1}	$\langle V \rangle\ <\ 0.313$ m ns^{-1}	–
	RMS(V) $<\ 0.08$ m ns^{-1}	RMS(V)/$\langle V \rangle < 0.08$	–
	Data: 1 January 2004 - 31 May 2010		$\geq 75\%$ of stations close to
	$\geq 60\%$ of stations with		shower core with ToT trigger
Young	ToT trigger & AoP > 1.4	Fisher discriminant based	&
Showers	Data: 1 June 2010 - 20 June 2013	on AoP of *early* stations	Fisher discriminant based
	$\langle$AoP$\rangle > 1.83$		on AoP of *early* stations
	AoP$_{\rm min} > 1.4$ if $N_{\rm st}$=3		close to shower core

Table I. Observables and numerical values of cuts applied to select *inclined* and *young* showers for Earth-skimming and downward-going neutrinos. See text for explanation.

2. *Combination of selections*

In previous publications [17, 18, 20] the fraction of ν-induced Monte Carlo events identified as neutrino candidates was obtained by applying each particular set of selection criteria (ES, DGH, DGL) only to its corresponding set of simulated showers (ES, DGH or DGL). In this work the fraction of selected events is further increased by applying the three sets of criteria to each sample of simulated showers (ES, DGH, DGL) regardless of channel. With this procedure the fraction of identified Monte Carlo events is enhanced as, for instance, an ES simulated shower induced by a ν_τ might not fulfill the requirements of the ES selection, but might still pass the DGH or DGL criteria, and hence contribute to the fraction of identified events. The enhancement in the fraction of events when applying this "combined" analysis depends on the particular set of Monte Carlo simulations. For instance applying the three criteria to the DGH Monte Carlo sample identifies a fraction of neutrino events ~ 1.25 larger than when the DGH criteria are applied alone, the enhancement coming mainly from events with 3 stations rejected by the DGH criteria but accepted by ES. The application of the three criteria to the ES Monte Carlo sample however results in a smaller enhancement ~ 1.04.

3. *Exposure calculation*

For downward-going neutrinos, once the efficiencies $\epsilon_{\rm DG}(E_\nu, \theta, D, t)$ are obtained, the calculation of the exposure involves folding them with the SD array aperture and the ν interaction probability at a depth D for a neutrino energy E_ν. This calculation also includes the possibility that downward-going ν_τ interact with the mountains surrounding the Observatory. Integrating over the parameter space except for E_ν and in time over the search periods and summing over all the interaction channels yields the exposure [18, 20].

In the Earth-skimming channel, $\epsilon_{\rm ES}(E_\tau, \theta, X_d)$ are also folded with the aperture, with the probability density function of a tau emerging from the Earth with energy E_τ (given a neutrino with energy E_ν crossing an amount of Earth determined by the zenith angle θ), as well as with the probability that the τ decays at an altitude X_d [17]. An integration over the whole parameter space except for E_ν and time gives the exposure [17].

The exposures $\mathcal{E}_{\rm ES}$, $\mathcal{E}_{\rm DGH}$ and $\mathcal{E}_{\rm DGL}$ obtained for the search periods of each selection are plotted in Fig. 3 along with their sum $\mathcal{E}_{\rm tot}$. The exposure to Earth-skimming neutrinos is higher than that to downward-going neutrinos, partially due to the longer search period in the Earth-skimming analysis, and partially due to the much larger neutrino conversion probability in the denser target of the Earth's crust compared to the atmosphere. The larger number of neutrino flavours and interaction channels that can be identified in the DGH and DGL analysis, as well as the broader angular range $60° < \theta < 90°$ partly compensates the dominance of the ES channel. The ES exposure flattens and then falls above $\sim 10^{19}$ eV as there is an increasing probability that the τ decays high in the atmosphere producing a no triggering shower, or even that the τ escapes the atmosphere before decaying. At the highest energies the DGH exposure dominates. The DGL exposure is the smallest of the three, mainly due to the more stringent criteria needed to apply to get rid of the larger background nucleonic showers in the zenith angle bin $60° < \theta < 75°$.

The relative contributions of the three channels to the total expected event rate for a differential flux behaving with energy as $dN_\nu(E_\nu)/dE_\nu \propto E_\nu^{-2}$ are ES:DGH:DGL$\sim$0.84:0.14:0.02 respectively, where the event rate is obtained as:

$$N_{\rm evt} = \int_{E_\nu} \frac{dN_\nu}{dE_\nu}(E_\nu)\ \mathcal{E}_{\rm tot}(E_\nu)\ dE_\nu \qquad (1)$$

C. Systematic uncertainties

Several sources of systematic uncertainty have been considered. Some of them are directly related to the Monte Carlo simulation of the showers, i.e., generator of the neutrino interaction either in the Earth or in the atmosphere, parton distribution function, air shower development, and hadronic model.

Other uncertainties have to do with the limitations on the theoretical models needed to obtain the interaction cross-section or the τ energy loss at high energies. In the Earth-skimming analysis the model of energy loss for the τ is the dominant source of uncertainty, since it determines the energy of the emerging τs after propagation in the Earth; the impact of this on the downward-going analysis is much smaller since τ energy losses are only relevant for ν_τ interacting in the mountains, a channel that is estimated to contribute only $\sim 15\%$ to the total exposure.

The uncertainty on the shower simulation, that stems mainly from the different shower propagation codes and hadronic interaction models that can be used to model the high energy collisions in the shower, contributes significantly in the ES and DG channels.

The presence of mountains around the Observatory – which would increase the target for neutrino interactions in both cases – is explicitly simulated and accounted for when obtaining the exposure of the SD to downward-going neutrino-induced showers, and as a consequence does not contribute directly to the systematic uncertainties. However, it is not accounted for in the Earth-skimming channel and instead we take the topography around the Observatory as a source of systematic uncertainty.

In the three channels the procedure to incorporate the systematic uncertainties is the same. Different combinations of the various sources of systematic uncertainty render different values of the exposure and a *systematic uncertainty band* of relative deviation from a reference exposure (see below) can be constructed for each channel and for each source of systematic uncertainty. For a given source of uncertainty the edges of the ES, DGH and DGL bands are weighted by the relative importance of each channel as given before and added linearly or quadratically depending on the source of uncertainty. In Table II we give the dominant sources of systematic uncertainty and their corresponding combined uncertainty bands obtained in this way. The combined uncertainty band is then incorporated in the value of the limit itself through a semi-Bayesian extension [21] of the Feldman-Cousins approach [22].

Source of systematic	Combined uncertainty band
Simulations	$\sim$ +4%, -3%
ν cross section & τ E-loss	$\sim$ +34%, -28%
Topography	$\sim$ +15%, 0%
Total	$\sim$ +37%, -28%

Table II. Main sources of systematic uncertainties and their corresponding combined uncertainty bands (see text for details) representing the effect on the event rate defined in Eq. (1). The uncertainty due to "Simulations" includes: interaction generator, shower simulation, hadronic model, thinning and detector simulator. The uncertainty due to "τ energy-loss" does not affect the DGL channel and only affects the DGH ν_τ with $\theta \gtrsim 88^\circ$ going through the mountains surrounding the Pierre Auger Observatory. The uncertainty due to "Topography" only affects the ES channel.

In the calculation of the reference exposure the ν-nucleon interaction in the atmosphere for DG neutrinos (including CC and NC channels) is simulated with HERWIG [23]. In the case of ν_τ CC interactions, a dedicated, fast and flexible code is used to simulate the τ lepton propagation in the Earth and/or in the atmosphere. The τ decay is performed with the TAUOLA package [24]. In all cases we adopted the ν-nucleon cross-section in [25]. In a second step, the AIRES code [26] is used to simulate the propagation of the particles produced in the high energy ν interaction or in the τ lepton decay. The types, energies, momenta and times of the particles reaching the SD level are obtained. The last stage is the simulation of the SD response (PMT signals and FADC traces). This involves a modification of the "standard" sampling procedure in [27] to regenerate particles in the SD stations from the "thinned" air shower simulation output, that was tailored to the highly inclined showers involved in the search for neutrinos. Light production and propagation inside the station is based on GEANT4 [28] with the modifications to account for the evolution of the light decay time explained above. These two latter changes roughly compensate each other, with the net result being a few percent decrease of the exposure with respect to that obtained with the standard thinning procedure and a constant average value of the light decay time.

IV. RESULTS

Using the combined exposure in Fig. 3 and assuming a differential neutrino flux $dN(E_\nu)/dE_\nu = k \cdot E_\nu^{-2}$ as well as a $\nu_e:\nu_\mu:\nu_\tau = 1:1:1$ flavour ratio, an upper limit on the value of k can be obtained as:

$$k = \frac{N_{\rm up}}{\int_{E_\nu}\ E_\nu^{-2}\ \mathcal{E}_{\rm tot}(E_\nu)\ dE_\nu}. \qquad (2)$$

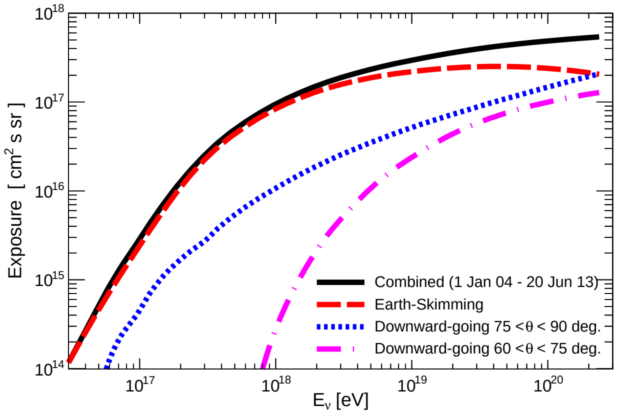

Figure 3. Combined exposure of the SD of the Pierre Auger Observatory (1 January 2004 - 20 June 2013) as a function of neutrino energy after applying the three sets of selection criteria in Table I to Monte Carlo simulations of UHE neutrinos (see text for explanation). Also shown are the individual exposures corresponding to each of the three selections. For the downward-going channels the exposure represents the sum over the three neutrino flavours as well as CC and NC interactions. For the Earth-Skimming channel, only ν_τ CC interactions are relevant.

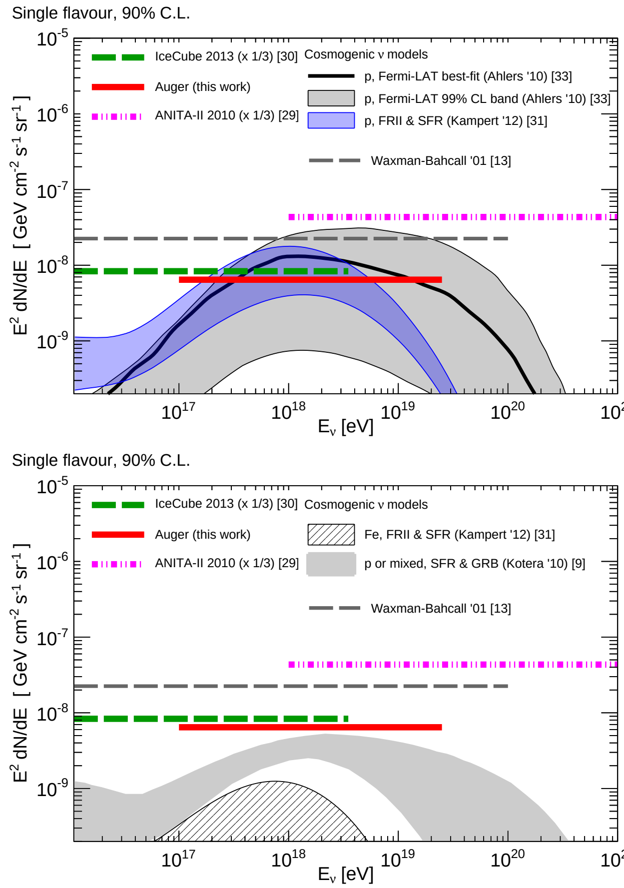

Figure 4. Top panel: Integrated upper limit (at 90% C.L.) from the Pierre Auger Observatory for a diffuse flux of UHE neutrinos. We also show the integrated limits from ANITAII [29] and IceCube [30] experiments, along with expected fluxes for several cosmogenic neutrino models that assume pure protons as primaries [31, 33] as well as the Waxman-Bahcall bound [13]. All limits and fluxes converted to single-flavour. We used $N_{\rm up} = 2.39$ in Eq. (2) to obtain the limit (see text for details). Bottom panel: Same as top panel, but showing several cosmogenic neutrino models that assume heavier nuclei as primaries, either pure iron [31] or mixed primary compositions [9].

The actual value of the upper limit on the signal events ($N_{\rm up}$) depends on the number of observed events (0 in our case) and expected background events (conservatively assumed to be 0), as well as on the confidence level required (90% C.L. in the following). Using a semi-Bayesian extension [21] of the Feldman-Cousins approach [22] to include the uncertainties in the exposure we obtain[3] $N_{\rm up} = 2.39$. The single-flavour 90% C.L. limit is:

$$k_{90} \;<\; 6.4 \times 10^{-9}\ \mathrm{GeV\ cm^{-2}\ s^{-1}\ sr^{-1}}. \qquad (3)$$

The limit applies in the energy interval $\sim 1.0 \times 10^{17}$ eV – 2.5×10^{19} eV where the cumulative number of events as a function of neutrino energy increases from 5% to 95% of the total number, i.e. where $\sim 90\%$ of the total event rate is expected. It is important to remark that this is the most stringent limit obtained so far with Auger data, and it represents a single limit combining the three channels where we have searched for UHE neutrinos. The limit in Eq. (3) is shown in Fig. 4 along with the integrated 90% C.L. limits from other experiments as well as several models of neutrino flux production (see caption for references). In Fig. 5 the limit is displayed in differential format [35], i.e. in different bins of width 0.5 in $\log_{10} E_\nu$ and expanding the energy range given before for the integrated limit. The differential limit allows us to show at which energies the sensitivity of the SD of the Pierre Auger Observatory peaks.

The search period corresponds to an equivalent of 6.4 years of a complete Auger SD array working continuously. The inclusion of the data from 1 June 2010 until 20 June 2013 in the search represents an increase of a factor ~ 1.8 in total time quantified in terms of equivalent full Auger years with respect to previous searches [17, 18]. Further improvements in the limit come from the combination of the three analysis into a single one, using the procedure explained before that enhances the fraction of identified neutrinos especially in the DGH channel.

In Table III we give the expected total event rates for several models of neutrino flux production.

Several important conclusions and remarks can be stated after inspecting Figs. 4 and 5 and Table III:

[3] To calculate $N_{\rm up}$ we use POLE++ [21]. The signal efficiency uncertainty is ~ 0.19 with an asymmetric band (see Table II). This yields a value of $N_{\rm up} = 2.39$ slightly smaller than the nominal 2.44 of the Feldman-Cousins approach.

Diffuse flux Neutrino Model	Expected number of events (1 January 2004 - 20 June 2013)	Probability of observing 0
Cosmogenic - proton, FRII [31]	~ 4.0	$\sim 1.8 \times 10^{-2}$
Cosmogenic - proton, SFR [31]	~ 0.9	~ 0.4
Cosmogenic - proton, Fermi-LAT [33]	~ 3.2	$\sim 4 \times 10^{-2}$
Cosmogenic - band [9]	$\sim 0.5 - 1.4$	$\sim 0.6 - 0.2$
Cosmogenic - iron, FRII [31]	~ 0.3	~ 0.7
Astrophysical ν (AGN) [32]	~ 7.2	$\sim 7 \times 10^{-4}$
Exotic [34]	~ 31.5	$\sim 2 \times 10^{-14}$

Table III. Number of expected events $N_{\rm evt}$ in Eq. (1) for several theoretical models of UHE neutrino production, given the combined exposure of the surface detector array of the Pierre Auger Observatory plotted in Fig. 3. The last column gives the Poisson probability $\exp(-N_{\rm evt})$ of observing 0 events when the number of expected events is $N_{\rm evt}$ given in the second column.

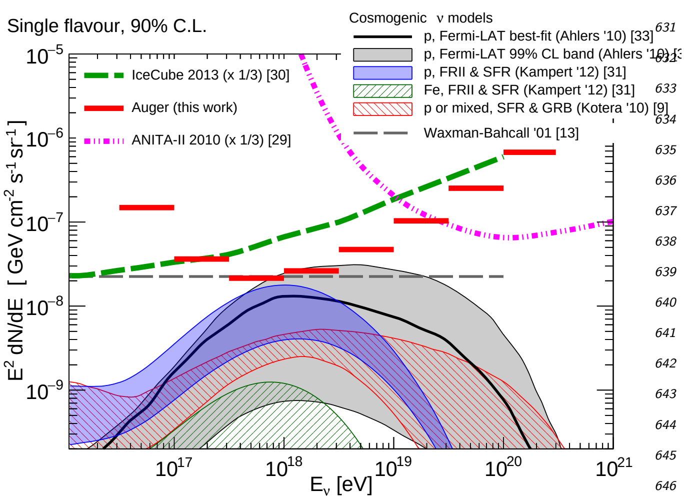

Figure 5. Differential upper limit (at 90% C.L. and in bins of width 0.5 in $\log_{10} E_\nu$) from the Pierre Auger Observatory for a diffuse flux of UHE neutrinos. We also show the differential limits from ANITAII [29] and IceCube [30] experiments, along with expected fluxes for several cosmogenic neutrino models [9, 31, 33] as well as the Waxman-Bahcall bound [13]. All limits and fluxes converted to single-flavour.

1. The maximum sensitivity of the SD of the Auger Observatory is achieved at neutrino energies around EeV, where most cosmogenic models of ν production also peak (in a $E_\nu^2 \times dN/dE_\nu$ plot).

2. The current Auger limit is a factor ~ 4 below the Waxman-Bahcall landmark on neutrino production in optically thin sources [13]. The SD of the Auger Observatory is the first air shower array to reach that level of sensitivity.

3. Some models of neutrino production in astrophysical sources such as Active Galactic Nuclei (AGN) are excluded at more than 90% C.L. For the model #2 shown in Fig. 14 of [32] we expect $\sim$7 neutrino events while none was observed.

4. Cosmogenic ν models that assume a pure primary proton composition injected at the sources and strong (FRII-type) evolution of the sources are strongly disfavored by Auger data. An example is the upper line of the shaded band in Fig. 17 in [31] (also depicted in Figs. 4 and 5), for which $\sim$4 events are expected and as consequence that flux is excluded at $\sim$98% C.L. Models that assume a pure primary proton composition and normalize their expectations to the GeV γ-ray flux observations by the Fermi-LAT satellite detector are also disfavored. For instance for the model shown as a solid line in the bottom right panel of Fig. 5 in [33] (also depicted in Figs. 4 and 5 in this work), corresponding to the best-fit to the cosmic-ray spectrum as measured by HiRes, we expect $\sim$3.2 events. As a consequence that model is excluded at more than 90% C.L. For this particular model we also show in Figs. 4 and 5 the 99% C.L. band resulting from the fitting to the HiRes spectrum down to 10^{19} eV. The Auger direct limits on cosmogenic neutrinos are also constraining part of the region indirectly bounded by Fermi-LAT observations.

5. The current Auger limit is less restrictive with the cosmogenic neutrino models represented by the gray shaded area in the bottom panel of Fig. 4 ($\sim$0.5 to $\sim$1.4 events are expected as shown in Table III) which brackets the lower fluxes predicted under a range of assumptions for the composition of the primary flux (protons or mixed), source evolution and model for the transition from Galactic to extragalactic cosmic-rays [9] The same remark applies to models that assume pure-iron composition at the sources. A 10-fold increase in the current exposure will be needed to reach the most optimistic predictions of cosmogenic neutrino fluxes if the primaries are pure iron, clearly out of the range of the current configuration of the Auger Observatory.

6. A large range of exotic models of neutrino production [34] are excluded with C.L. larger than 99%.

7. In IceCube, neutrino fluxes in the 30 TeV to 2 PeV

energy range have shown a $\sim$5.7σ excess compared to predicted atmospheric neutrino fluxes [12]. A refinement of the IceCube search technique to extend the neutrino sensitivity down to 10 TeV [36], yielded a power-law fit to the measured flux without cut-off given by $dN/dE = \Phi_0(E_\nu/E_0)^{-\gamma}$ with $\Phi_0 = 2.06\times10^{-18}$ GeV^{-1} cm^{-2} s^{-1} sr^{-1}, $E_0 = 10^5$ GeV, and $\gamma = 2.46$. If this flux is extrapolated to 10^{20} eV it would produce $\sim$0.1 events in Auger.

V. ACKNOWLEDGMENTS

The successful installation, commissioning, and operation of the Pierre Auger Observatory would not have been possible without the strong commitment and effort of the technical and administrative staff in Malargüe.

[1] R. U. Abbasi *et al.* [HiRes Collaboration], Phys. Rev. Lett. **100**, 101101 (2008).

[2] J. Abraham *et al.* [Pierre Auger Collaboration], Phys. Rev. Lett. **101**, 061101 (2008); J. Abraham *et al.* [Pierre Auger Collaboration], Phys. Lett. B **685**, 239 (2010).

[3] K. Greisen, Phys. Rev. Lett. **16**, 748 (1966); G. T. Zatsepin and V. A. Kuzmin, Pis'ma ZhZhurnal Eksperimental noi i Teoreticheskoi Fiziki **4**, 114 (1966), JETP Lett. **4**, 78 (1966) (Engl. Transl.).

[4] D. Allard, Astropart. Phys. **33**, 39 (2012).

[5] P. Abreu *et al.* [Pierre Auger Collaboration], Phys. Rev. Lett. **104**, 091101 (2010); A. Aab *et al.* [Pierre Auger Collaboration], arXiv:1409.4809 [astro-ph].

[6] R. U. Abbassi *et al.* [Telescope Array Collaboration] Astropart. Phys. **64**, 49 (2015).

[7] V. S. Berezinsky and G. T. Zatsepin, Phys. Lett. B **28**, 423 (1969).

[8] D. Hooper *et al.*, Astropart. Phys. **23**, 11 (2005) 11; M. Ave *et al.*, Astropart. Phys. **23**, 19 (2005) 19.

[9] D. Allard *et al.*, JCAP **10**, 013 (2010).

[10] D. Seckel and T. Stanev, Phys. Rev. Lett. **95**, 141101 (2005).

[11] J. K. Becker, Phys. Rep. **458**, 173 (2008).

[12] M. G. Aartsen *et al.* [IceCube Collab.] Phys. Rev. Lett. **113**, 101101 (2014).

[13] E. Waxman and J. N. Bahcall, Phys. Rev. D **59**, 023002 (1998); Phys. Rev. D **64**, 023002 (2001).

[14] B. Baret and V. Van Elewyck, Rep. Prog. Phys. **74**, 046902 (2011).

[15] J. Abraham *et al.* The Pierre Auger Collab., Nucl. Instrum. Meth. A **523**, 50 (2004).

[16] J. Abraham *et al.* [Pierre Auger Collaboration], Nucl. Instrum. Meth. A **613**, 29 (2010).

[17] J. Abraham *et al.* [Pierre Auger Collab.], Phys. Rev. Lett. **100**, 211101 (2008); J. Abraham *et al.* [Pierre Auger Collab.], Phys. Rev. D **79**, 102001 (2009); P. Abreu *et al.* [Pierre Auger Collab.], Astrophys. J. Lett. **755**, L4 (2012).

[18] P. Abreu *et al.* [Pierre Auger Collab.], Phys. Rev. D **84**, 122005 (2011).

[19] R. Fisher, Ann. Eugenics **7**, 179 (1936).

[20] J. L. Navarro, PhD Thesis, Univ. Granada, Spain (2012).

[21] J. Conrad *et al.*, Phys. Rev. D **67**, 012002 (2003).

[22] G. J. Feldman, R. D. Cousins, Phys. Rev. D **57**, 3873 (1998).

[23] G. Corcella *et al.*, HERWIG 6.5, JHEP **01**, 010 (2001).

[24] S. Jadach *et al.*, Comput. Phys. Commun. **76**, 361 (1993).

[25] A. Cooper-Sarkar, S. Sarkar, JHEP **0801**, 075 (2008).

[26] S. J. Sciutto, arXiv:astro-ph/9911331 http://www2.fisica.unlp.edu.ar/auger/aires/ppal.html

[27] P. Billoir, Astropart. Phys. **30**, 270 (2008).

[28] http://geant4.cern.ch/

[29] P. W. Gorham *et al.* [ANITA Collab.], Phys. Rev. D **85**, 049901(E) (2012).

[30] M. G. Aartsen *et al.* [IceCube Collab.] Phys. Rev. D **88**, 112008 (2013).

[31] K. -H. Kampert, M. Unger, Astropart. Phys. **35**, 660 (2012).

[32] J. K. Becker, P.L. Biermann, W. Rhode, Astropart. Phys. **23**, 355 (2005).

[33] M. Ahlers *et al.*, Astropart. Phys. **34**, 106 (2010).

[34] O. Kalashev *et al.*, Phys. Rev. D **66**, 063004 (2002).

[35] L. A. Anchordoqui *et al.*, Phys. Rev. D **66**, 103002 (2002)

[36] M. G. Aartsen *et al.* [IceCube Collab.] Phys. Rev. D **91**, 022001 (2015).